Accepted Manuscript

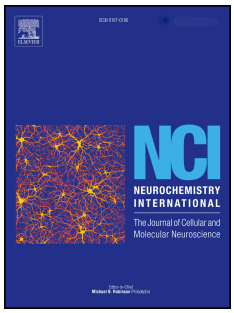

HPOB, an HDAC6 inhibitor, attenuates corticosterone-induced injury in rat adrenal pheochromocytoma PC12 cells by inhibiting mitochondrial GR translocation and the intrinsic apoptosis pathway

Zong-yang Li, Qing-zhong Li, Lei Chen, Bao-dong Chen, Ce Zhang, Xiang Wang, Wei-ping Li

PII: S0197-0186(16)30081-X

DOI: 10.1016/j.neuint.2016.08.004

Reference: NCI 3903

To appear in: *Neurochemistry International*

Received Date: 4 May 2016

Revised Date: 4 August 2016

Accepted Date: 10 August 2016

Please cite this article as: Li, Z.-y., Li, Q.-z., Chen, L., Chen, B.-d., Zhang, C., Wang, X., Li, W.-p., HPOB, an HDAC6 inhibitor, attenuates corticosterone-induced injury in rat adrenal pheochromocytoma PC12 cells by inhibiting mitochondrial GR translocation and the intrinsic apoptosis pathway, *Neurochemistry International* (2016), doi: 10.1016/j.neuint.2016.08.004.

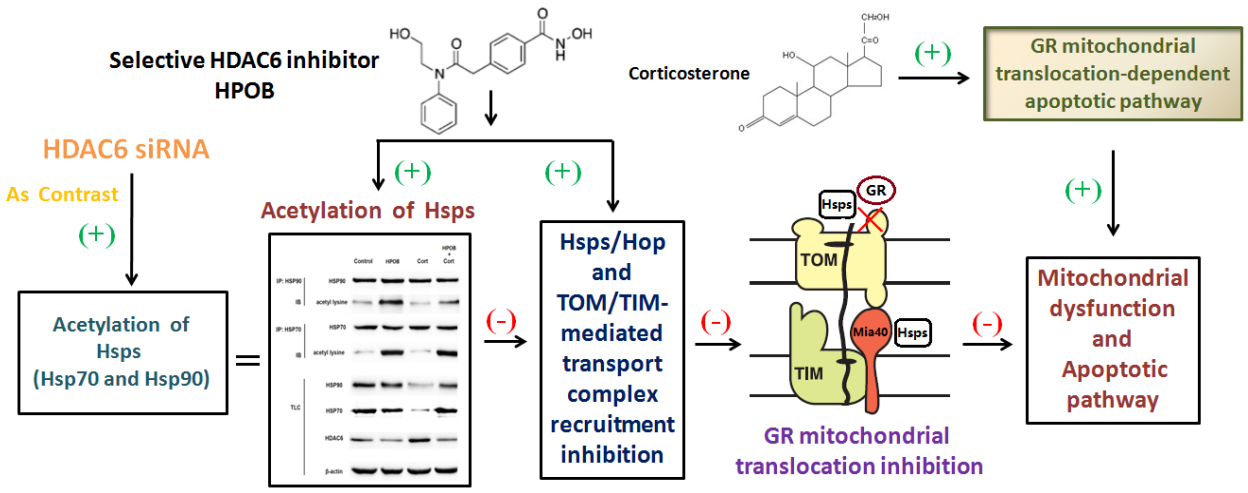

HPOB, an HDAC6 inhibitor, attenuates corticosterone-induced injury in rat adrenal pheochromocytoma PC12 cells by inhibiting mitochondrial GR translocation and the intrinsic apoptosis pathway

Zong-yang Li [1,a], Qing-zhong Li [1,b], Lei Chen [a], Bao-dong Chen [a], Ce Zhang [a], Xiang Wang [a], Wei-ping Li*, [a]

[a] Brain center, Shenzhen Key Laboratory of Neurosurgery, Shenzhen Second People's Hospital, Shenzhen University 1st Affiliated Hospital, Shenzhen 518035, China
[b] Shantou University Medical College, Shantou 515041, China

[1] Zong-yang Li and Qing-zhong Li contributed equally to this work.
*Corresponding author: Brain Center, Shenzhen Key Laboratory of Neurosurgery, Shenzhen Second People's Hospital, Shenzhen University 1st Affiliated Hospital, #3002 Sungang Road, Futian District, Shenzhen 518035, China. Tel.: (86)-0755-83792752
E-mail address: wpli@szu.edu.cn

Abstract

High levels of glucocorticoids (GCs) have been reported to damage normal hippocampal neurons, and such damage has been positively correlated with major depression (MD) and chronic stress. Our previous study showed that HDAC6 might be a potential target to regulate GC-induced glucocorticoid receptor (GR) translocation to the mitochondria and subsequent apoptosis. In the present study, we investigated the effect of HPOB, a selective HDAC6 inhibitor, on corticosterone (Cort)-induced apoptosis and explored the possible mechanism of action of HPOB in rat adrenal pheochromocytoma (PC12) cells, which possesses typical neuron features and expresses high levels of glucocorticoid receptors. We demonstrated that pre-treatment with HPOB remarkably reduced Cort-induced cytotoxicity and confirmed the anti-apoptotic effect of HPOB via the caspase-3 activity assay and H33342/PI and TUNEL double staining. Mechanistically, we demonstrated that HPOB reversed the Cort-induced elevation of GR levels in the mitochondria and blocked concomitant mitochondrial dysfunction and the intrinsic apoptosis pathway. Furthermore, HPOB was shown to attenuate expression of the multi-chaperone

machinery (Hsp90-Hop-Hsp70) and cooperate with mitochondrial translocase of the outer/inner membrane (TOM/TIM) complex recruitment by triggering hyperacetylation of Hsps through HDAC6 inhibition. Considering all of these findings, the neuroprotective effect of HPOB demonstrated the crucial role of HDAC6 inhibition in reducing Cort-induced apoptosis in PC12 cells. The data further suggested that the anti-apoptotic activity of HDAC6 inhibition against the mitochondria-mediated impairment pathway might be mechanistically linked to the hyperacetylation of Hsps and consequent suppression of GR translocation to the mitochondria.

Keywords

HDAC6; HPOB; glucocorticoid receptor; mitochondrial translocation; Hsp90

Abbreviations

Cort, corticosterone; DRP1, dynamin-related protein 1; Fis1, mitochondrial fission molecule 1; GCs, glucocorticoids; GR, glucocorticoid receptor; HDACs, histone deacetylases; Hsps, heat-shock proteins; Map-1, modulator of apoptosis-1; MD, major depression; MMP, mitochondrial membrane potential; mPTP, mitochondrial permeability transition pore; mtHsps, mitochondrial Heat-shock proteins; Tom, translocation complexes of outer membrane; VDAC protein, voltage-dependent anion-selective channel protein.

1. Introduction

Glucocorticoids (GCs) belong to the family of steroid hormones that regulate a variety of physiological processes, including energy metabolism, inflammation and stress responses (Tang et al., 2013). As part of the stress response, chronic elevation of circulating GCs is a harmful stimulus that affects the function of the central nervous system (CNS). GC-induced apoptosis has been regarded as a principal factor inducing reduction of hippocampal volume, which is considered the crucial

characteristic of patients with major depression (MD) and chronic stress (Sapolsky, 2000). The effects of GCs are predominantly mediated through interaction with the glucocorticoid receptor (GR). These receptors are ubiquitous ligand-dependent transcription factors that regulate gene expression through either trans-activation or trans-repression of gene targets (Mikosz et al., 2001; Savoldi et al., 1997). Under normal conditions, GRs are localized primarily within the cytosolic fraction in an unoccupied resting state. However, upon treatment with an agonist or under stress conditions, GRs become progressively occupied and rapidly translocate to the nucleus, where they initiate or modify gene transcription (He et al., 2002; Maiyar et al., 1997). However, recent studies have reported that a sub-fraction of GRs can be detected in the mitochondria in liver and brain cell lines, suggesting that the mitochondria may function as an alternative non-genomic site of the genomic action of GCs (Demonacos et al., 1995; Moutsatsou et al., 2001; Psarra and Sekeris, 2011). Furthermore, several studies have suggested mitochondrial GR translocations are regulated differently from nuclear GRs and may induce apoptosis independently or collaboratively with nuclear GR effects (Du et al., 2009; Sionov et al., 2006a).

Mitochondria play crucial roles in several cellular processes, including energy production, programmed cell death, signalling, and metabolic pathways. During apoptosis, mitochondria orchestrate programmed cell death through the intrinsic pathway and the release of pro-apoptotic proteins (Adzic et al., 2009). Elevated GC levels have been demonstrated to influence the functions of mitochondria, and GCs may independently mediate the elevation of resting metabolic rates during severe injury or stress (Moutsatsou et al., 2001). Furthermore, previous findings from our group revealed that saikosaponin D (an oleanane-type glycoside) could reverse Cort-induced apoptosis through blocking the mitochondrial translocation of GR, indicating that mitochondrial GR translocation might be both essential for GC-induced apoptosis and independent of the nuclear effects of GRs (Li et al., 2014). Therefore, it could be hypothesized that mitochondrial GR translocation-induced apoptosis might be an important component of the biochemical changes and injuries that occur after GC exposure under MD or chronic stress circumstances.

Mitochondrial GR translocation might also be considered as a target for therapeutic modalities against GC-induced neuronal apoptosis.

Our work found that histone deacetylase 6 (HDAC6) and heat shock protein 90 (Hsp90) were probably associated with mitochondrial GR translocation, as the reduction of HDAC6 and reinforcement of Hsp90 may contribute to its inhibition (Li et al., 2014). HDAC6 is the principal member of the histone deacetylase (HDAC) family and is actively and stably maintained in the cytoplasm. HDAC6 has been demonstrated to be involved in cell survival, invasion, tumorigenesis and cellular responses to proteotoxic stress via post-translational modifications (Kovacs et al., 2005). Importantly, HDAC6 plays an important role in regulating the deacetylation of molecular chaperones in the cytoplasm. Hsp90 is a confirmed substrate of HDAC6, and its chaperone activity is regulated by HDAC6 (Namdar et al., 2010; Rao et al., 2012; Ryhanen et al., 2011). These investigations indicate that the regulation of HDAC6-mediated post-translational modifications of Hsps might inhibit GR mitochondrial translocation, thereby blocking GC-induced neuronal apoptosis. To test this hypothesis, we explored the influence and mechanisms of HDAC6 inhibition in Cort-induced apoptosis.

N-hydroxy-4-(2-[(2-hydroxyethyl) (phenyl)amino]-2-oxoethyl) benzamide (HPOB) is a hydroxamic acid-based small-molecule HDAC6 inhibitor. It selectively inhibits HDAC6 catalytic activity in vivo and in vitro with an IC_{50} of 56 nM but does not block the ubiquitin-binding activity of HDAC6. Furthermore, HPOB was shown to increase the effectiveness of etoposide, doxorubicin, and SAHA anticancer agents in inducing cell death of transformed cells but not normal cells (Lee et al., 2013). In the present study, we report that treatment of rat adrenal pheochromocytoma (PC12) cells with HPOB reversed Cort-induced GR mitochondrial translocation and apoptosis through the intrinsic mitochondrial pathway. PC12 cell line, which possesses typical neuron features and expresses high levels of glucocorticoid receptors, is one of the widely used neuronal cell lines in a variety of studies. Based on the involvement of HPOB in the switch towards a pro-survival effect, we provide novel insight into the role of HDAC6-dependent deacetylation of Hsp90, which disturbs the translocation of

GRs into the mitochondria. Notably, HPOB treatment triggered dramatic hyperacetylation of Hsps, restricted the binding of Hsp90 to Tom70 and Hop, decreased the levels of Tim22, Mia40 and mitochondrial Hsp60 (mtHsp60), and resulted in the obstruction of co-chaperone-dependent mitochondrial transmembrane transport, which ultimately blocked mitochondrial GR translocation. Moreover, we found a correlation between mitochondrial GR translocation and GC-induced apoptosis. When GR mitochondrial translocation was reversed by HPOB, the abnormal opening of the mitochondrial permeability transition pore (mPTP) and depolarisation of the mitochondrial transmembrane potential (MMP) were ameliorated, and the intrinsic mitochondria fission and apoptotic pathways were also blocked. Therefore, we concluded that HPOB-induced inhibition of HDAC6 might be a potential target for blocking GC-induced apoptosis.

2. Materials and methods

2.1 Materials

HPOB used in cell culture experiments was purchased from Selleck Chemicals (HOU, USA). Foetal bovine serum (FBS), heat-inactivated horse serum, penicillin, and streptomycin were purchased from Gibco (Grand Island, NY, USA). Dimethyl sulfoxide (DMSO), Dulbecco's Modified Eagle Medium (DMEM), corticosterone (Cort) and thiobarbituric acid were obtained from Sigma-Aldrich (St. Louis, MO, USA). The following primary antibodies were purchased from Santa Cruz Biotechnology (CA, US): antibodies to GAPDH (1:1000), Fis1 (1:500), DRP1 (1:500), cytochrome c (1:500), GR (1:500), HDAC6 (1:500), histone H2B (1:500), α-tubulin (1:1000), and VDAC (voltage-dependent anion-selective channel) protein (1:500). The following primary antibodies were purchased from Abcam (UK): primary antibodies to Hsp90 (heat-shock protein 90) (1:500), Hsp70 (heat-shock protein 70) (1:200), Hsp60 (heat-shock protein 60) (1:200), Tom20 (translocation complexes of outer membrane 20) (1:200), Tom40 (1:200), Tom70 (1:200), Tim 22 (translocation complexes of inner membrane 22) (1:200), Hop (Hsp70/Hsp90-organizing protein),

and Mia40 (1:200). Goat anti-mouse secondary antibodies labelled with horseradish peroxidase were also purchased from Abcam. A monoclonal anti-acetyl lysine antibody was purchased from Cell Signaling Technology (Beverly, MA). All other chemicals and reagents were analytical grade.

2.2. Cell culture and drug treatments

PC12 and SH-SY5Y neuroblastoma cells were obtained from the Chinese Academy of Medical Sciences and cultured in vitro. PC12 cells were grown in DMEM supplemented with 10% (v/v) foetal bovine serum, 5% (v/v) heat-inactivated horse serum, 100 U/ml penicillin, and 100 μg/ml streptomycin. Cells were cultured in a humidified atmosphere of 95% air and 5% CO_2 at 37 °C. SH-SY5Y cells were grown in DMEM supplemented with 10% (v/v) foetal bovine serum, 100 U/ml penicillin, and 100 μg/ml streptomycin. Cells were cultured in a humidified atmosphere of 95% air and 5% CO_2 at 37 °C. Cells in the exponential growth phase were used for all experiments. HPOB was first dissolved in DMSO at a concentration of 10 mM and then in DMEM (0.1-2 μM) immediately before use. Final preparations contained less than 0.1% (v/v) DMSO. As evidenced by comparisons with vehicle-free control medium, DMSO had no toxic effect on cell viability and did not affect the assays. To study the anti-apoptotic effect of HPOB, the cells were divided into untreated control, HPOB alone, Cort (250 μM), and Cort (250 μM) plus HPOB groups. Cells were pre-incubated with HPOB for 24 h and then co-treated with Cort for 24 h, while the untreated control group was treated with the appropriate amount of vehicle.

2.3. Measurement of lactate dehydrogenase (LDH) release

The cell damage was determined by the release of lactate dehydrogenase (LDH) into the incubation medium using the assay kit (Nanjing Jiancheng Bioengineering Institute, China) according to the manufacturer's instructions. Briefly, after the treatment, the cells in 6-well plate were centrifuged at 1000g for 4 min, 1 mL culture supernatants were collected from each well; 3.4 mL reaction buffer supplied in the kit

was then added. 30 min after mixing at room temperature, the release of LDH was assessed using a microplate reader at a test wavelength of 340 nm and expressed as a percentage (%) of total LDH activity (LDH in the medium + LDH in the cell), according to the equation % LDH released = (LDH activity in the medium/total LDH activity) × 100. Each experiment was performed for four times.

2.4. Caspase-3 activity determination

Cells were harvested by centrifugation and the media removed. A volume of 50 μl of 10 μM substrate solution (PhiPhilux is a unique class of substrates for caspase-3) was added to the cell pellet (1×10^5 cells per sample); the cells were not vortex mixed. Cells were incubated at 37℃ for 60 minutes, then washed once by adding 1 ml of ice-cold PBS and were re-suspended in 1 ml fresh PBS. Cells were analyzed with a flow cytometer (Becton-Dickinson) equipped with an argon ion laser at 488 nm wavelength. Caspase-3 activity was determined and analyzed.

2.5. H33342 /Propidium Iodide Staining

Furthermore, Hoechst 33342 and PI double fluorescent staining was assayed. Annexin V/propidium iodide (PI) assay kits were purchased from Invitrogen (Eugene, OR, USA). The cells were cultured on coverslips in 24-well plates for 24 h. After the treatment, the cells were incubated with 5 mg/ml Hoechst 33342 for 15 min, washed twice with PBS, incubated with 1 μg/ml PI working solution for an additional 15 min, and then visualised by inverted fluorescence microscopy (Leica, Germany). The apoptotic nuclei were counted in at least 200 cells from five randomly selected fields in each treatment and are expressed as percentages of the total numbers of counted nuclei.

2.6. Measurement of DNA fragmentation

The DNA fragmentation of apoptotic PC12 cells was detected using a terminal deoxynucleotidyl transferase-mediated biotinylated UTP nick end labelling (TUNEL)

kit (Roche Diagnostics Corp., IN, USA). The cells were cultured on coverslips for 24 h. At the end of the drug treatment, the cells were fixed by incubation in a 10% neutral buffered formalin solution for 30 min at room temperature. Next, the cells were incubated with a methanol solution containing 0.3% H_2O_2 for 30 min at room temperature and then incubated with a permeabilising solution (0.1% sodium citrate and 0.1% Triton X-100) for 2 min at 4 °C. The cells were incubated with the TUNEL reaction mixture for 60 min at 37 °C and visualized by inverted fluorescence microscopy (Leica, Germany). The TUNEL-positive nuclei of four non-overlapping fields per coverslip were counted, and these counts were converted to percentages by comparing the TUNEL-positive counts to the total numbers of cell nuclei, as determined by DAPI counterstaining.

2.7. Subcellular fractionation

Cell pellets were gently resuspended in cytoplasmic buffer (10 mM Hepes, pH 7.4; 1.5 mM $MgCl_2$, 10 mM KCl, 0.5 mM DTT, 10 mM Na2MoO_4, 2 mM PMSF, 20 μg/ml aprotinin, 0.1% NP-40; 25 mM NaF, and 0.2 mM Na_3VO_4) and kept on ice for 10 min before centrifugation at 900 g for 10 min. The nuclear pellets were processed as described below. The cytoplasmic supernatant was re- centrifuged at 900 g to ensure complete removal of nuclear material. The resulting supernatant was centrifuged at 10,000 g for 30 min. The cytosolic supernatant was processed for Western blot by adding protein sample buffer (PSB) × 4.5. The mitochondrial pellet was washed with cytoplasmic buffer, recentrifuged at 10,000 g, and dissolved in PSB × 1.5. The nuclear pellet was washed with cytoplasmic buffer and recentrifuged at 900 g before their extraction in nuclear buffer (20 mM Hepes, pH 7.4, 1.5 mM $MgCl_2$, 420 mM NaCl, 25% glycerol (vol/vol), 0.2 mM EDTA, 0.5 mM DTT, 10 mM Na_2MoO_4, 2 mM PMSF, 20 μg/ml aprotinin, 25 mM NaF, and 0.2 mM Na_3VO_4). The nuclear extracts were cleared at 20,000 g for 10 min, and processed for Western blot by adding PSB × 4.5. The Oncogene cytosol/mitochondria fractionation kit (QIA88; Oncogene Research Products) was used according to the manufacturer's instructions.

2.8. Measurement of mitochondrial permeability transition pore (mPTP) opening

The opening of the mPTP in Cort-treated PC12 cells was determined using the calcein-cobalt quenching Detection Kit (Genmed Scientifics, Inc.). All procedures completely complied with the manufacturer's instructions. The cells were cultured in 24-well plates. After the indicated treatments, PC12 cells were loaded with calcein dye and in the presence of cobalt chloride ($CoCl_2$ 1 mmol/L) at 37 ℃ for 30 min. Images were acquired using a Leica fluorescence microscope (Leica, Germany) with excitation and emission wavelengths of 488 and 505 nm, respectively. The opening of mPTP in each group was calculated as the fluorescence intensity. The opening of mPTP was analysed using a fluorescence microplate reader after calcein-cobalt staining. The results are expressed as a percentage of control.

2.9. Measurement of mitochondrial membrane potential (MMP)

5,5',6,6'-tetrachloro-1,1',3,3'-tetraethylbenzimidazolyl-carbocyanine iodide (JC-1, Invitrogen, Eugene, OR, USA) was used to determine the changes in MMP in the corticosterone-treated PC12 cells. Briefly, the cells were suspended in warm medium at approximately 1×10^6 cells/ml and then incubated with JC-1 (2 mM final concentration) for 30 min in the dark. After incubation, the cells were washed twice with PBS and visualised using a fluorescence microscope (Leica, Germany). Monomeric JC-1 green fluorescence emission and aggregate JC-1 red fluorescence emission were measured on a microplate reader. The MMP of the PC12 cells in each treatment group were calculated as the ratios of red to green fluorescence.

2.10. Western blot analyses and immunoprecipitation

At the end of the treatments, PC12 cells were harvested and washed once with PBS. The cells to be used for protein analysis were lysed with a cell lysis buffer containing 1% phenylmethylsulfonylfluoride (PMSF). Whole cell lysates were centrifuged at 12,000 rpm for 5 min at 4 °C, and the supernatant was collected. The protein

concentration was determined using a bicinchoninic acid assay. Equal amounts of protein (10 μg) were separated by electrophoresis on 10% sodium dodecyl sulfate polyacrylamide gels and transferred onto nitrocellulose membranes. These membranes were incubated with 5% (w/v) non-fat milk powder in Tris-buffered saline containing 0.1% (v/v) Tween-20 (TBST) for 40 min to block nonspecific binding sites. The membranes were then incubated overnight at 4 °C with the primary antibodies. After washing with TBST, the membranes were incubated for 1 h at room temperature with the secondary antibodies. After rewashing with TBST, the bands were developed by enhanced chemiluminescence. Immunoprecipitation of Hsp90, Hsp70, Hop, and Tom70 were carried out using specific-antibodies and immunoblotted with anti-Hsp90, Hsp70, Hop, Tom70 or anti–acetyl lysine antibodies, respectively. Class-specific IgG antibodies were used as controls in the immunoprecipitation experiments. Horizontal scanning densitometry was performed on western blots using Adobe PhotoShop (Adobe Systems, Inc.)

2.11. Transfections

PC12 cells were transiently transfected according to the manufacturer's instructions using Lipofectamine and Plus Reagent (Invitrogen) with plasmids containing a scrambled oligonucleotide (control siRNA). For HDAC6 knockdown, PC12 cells were transfected with PBS/U6 (control vector) with or without the HDAC6 small interfering RNA (siRNA), which contains a 21-nucleotide sequence 5'-GGATGGATCTGAACCTTGAGA-3' corresponding to the targeted nucleotides (200 to 219) in the HDAC6 mRNA.

2.12. Statistical analysis

Results are represented as the means ± the standard deviations (SDs) for each experimental group. The data were analysed by one-way ANOVA followed by a post hoc Tukey test to compare the control and treatment groups; p-values less than 0.05 were considered as statistically significant. All statistical analyses were performed

with the SPSS17.0 software. All experiments were performed a minimum of three times.

3. Results

3.1. Effect of HPOB on GCs-induced apoptosis in PC12 and SH-SY5Y cells

First, the effects of HPOB at different concentrations on Cort-treated PC12 cells were measured using the CCK-8 assay. The results showed that HPOB treatment alone (0.01-4 μM) did not alter cell viability (Fig. 1A). However, pre-treatment with HPOB resulted in a significant decrease in Cort-induced toxicity in a dose-dependent manner, and 0.5 μM of HPOB showed the best neuroprotection (Fig. 1B). Furthermore, LDH release and caspase-3 activity were measured to confirm the anti-apoptotic effect of HPOB on Cort-treated PC12 cells. As shown in Fig. 1C and D, pre-treatment of HPOB at the indicated concentrations distinctly attenuated the Cort-induced upregulation of LDH release and caspase-3 activity in a dose-dependent manner. Again, 0.5 μM of HPOB exerted the strongest neuroprotection. In addition, we further checked the anti-apoptotic effect of HPOB against Glucocorticoids-induced apoptosis in human neuroblastoma SH-SY5Y cells. The results confirmed pretreatment with HPOB reversed dexamethasone-induced decrease in viability of SH-SY5Y cells (Fig. 1E-G), and attenuated dexamethasone-induced increase in LDH release of SH-SY5Y cells (Fig. 1H). Notably, the dose-dependent neuroprotection of HPOB only ranged from 0.01 μM to 0.5 μM; higher concentrations of HPOB (2 and 4 μM) were actually less protective against Cort-induced toxicity, probably due to off-target or excessive HDAC6 inhibition of HPOB. These results indicated moderate inhibition of HDAC6 might be beneficial for survival. To further investigate the possible mechanism of HPOB protection against Cort-induced toxicity, a 0.5 μM HPOB concentration was selected for subsequent experiments.

Fig. 1. Effects of HPOB on GCs-induced apoptosis in PC12 and SH-SY5Y cells. (A) Effect of 48 h

treatment with HPOB alone and (B) anti-apoptotic effect of HPOB pre-treatment for 24 h on Cort-induced apoptosis in PC12 cells. (C) Effect of HPOB pre-treatment for 24 h on LDH leakage. (D) Effect of HPOB pre-treatment for 24 h on caspase-3 activity. (E) Effect of 24 h treatment with Dexamethasone (DEX) at the indicated concentration on the viability SH-SY5Y cells. (F) Effect of 48 h treatment with HPOB alone on the viability SH-SY5Y cells and (G) anti-apoptotic effect of HPOB pre-treatment for 24 h on DEX-induced apoptosis in SH-SY5Y cells. (H) Effect of HPOB pre-treatment for 24 h on LDH leakage. The results are expressed as the means ± SD of three independent experiments. ## indicates a significant difference from the control ($P < 0.01$). * indicates a significant difference from treatment with Cort alone at $P < 0.05$. ** indicates a significant difference from treatment with Cort alone at $P < 0.01$.

3.2. HPOB attenuated Cort-induced apoptosis in PC12 cells

We further examined the effects of HPOB on Cort-induced apoptosis via Hoechst 33342/PI and DAPI/TUNEL double staining. As shown in Fig. 2A and C, a markedly higher number of PI-positive cells were detected in cultures treated with Cort than in control cells, while there was about 50% reduction of PI-positive cells in the HPOB+Cort condition compared to the Cort condition. In addition, the number of TUNEL-positive cells increased significantly in cultures treated with Cort compared to control cells, while there was approximately a 50% reduction of TUNEL-positive cells in the HPOB+Cort condition compared to the Cort condition. (Fig. 2C and D).

Fig. 2. The effects of HPOB on cell survival in Cort-treated PC12 cells as determined using TUNEL staining. (A) Representative images of Hoechst 33342/PI double staining, including representative images of PI-positive cells (red, apoptotic cells) and Hoechst counterstaining (blue, normal cells). Scale bar: 400 μm. (B) Representative images of TUNEL-positive cells (green, middle row) and DAPI counterstaining (blue, top row). Scale bar: 200 μm. (C) Quantification of PI-positive staining. (D) Quantification of TUNEL staining. The histogram shows the relative proportion of PI-positive and TUNEL-positive cells in different treatment groups. Cells were pre-incubated with HPOB for 24 h and

then co-treated with Cort for 24 h. The untreated control group was incubated with the appropriate amount of vehicle. The results are expressed as the means ± SD (n=3). ##P<0.01 compared with the control group; **P<0.01 compared with corticosterone group.

3.3. Effect of HPOB on the translocation of GR

PC12 cells were incubated and divided into untreated control, Cort, and Cort plus HPOB groups, and the subcellular fractions were separated using the procedure above and a mitochondria fractionation kit before subjecting fractions to western blotting. Cross-contamination among the nuclear, cytosolic, and mitochondrial fractions was ruled out using antibodies against histone H2B, α-tubulin, and VDAC that react with nuclear, cytosolic, and mitochondrial fractions, respectively (Fig. 3B). VDAC could be used as a mitochondrial marker because the cells were harvested before mitochondrial fission. The mitochondrial fraction was not contaminated with cytosolic or nuclear proteins. As shown in Fig. 3A, Cort treatment reinforced mitochondrial and nuclear GR translocation in PC12 cells compared with the control group, and HPOB inhibited this effect. However, the amount of nuclear GR did not decrease significantly. Interestingly, pre-treatment with HPOB enhanced cytosolic retention of GR compared with the Cort group, while treatment with HPOB alone did not alter the levels of GR in the different sub-fractions compared with the control group. This observation highlighted the need to study GR trafficking in the context of the GC-dependent pathway.

Fig. 3. HPOB treatment altered intracellular distribution of GR and inhibited the mitochondrial translocation of GR in PC12 cells (Cort group). (A) GR was detected using western blotting with an anti-GR antibody. The blots were probed with antibodies specific for α-tubulin (cytoplasm), histone H2B (nuclear), VDAC (mitochondria) and β-actin (cell lysis). HPOB inhibited the increased translocation of GR to the mitochondria but not to the nucleus of PC12 cells (HPOB + Cort group). (B)

The mitochondrial fraction was not contaminated by cytosolic or nuclear proteins. Subcellular fractions were analysed using western blotting with antibodies specific for α-tubulin, histone 2B, and VDAC to react with cytosolic, nuclear, and mitochondrial fractions, respectively. Protein levels were quantified using densitometry. Cells were pre-incubated for 24 h with HPOB and then co-treated with Cort for 18 h. The untreated control group was incubated with the appropriate amount of vehicle. The results are expressed as the means ± SD (n=3). ## indicates a significant difference from the control at $P < 0.01$. * indicates a significant difference from treatment with Cort alone at $P < 0.05$). ** indicates a significant difference from treatment with Cort alone at $P < 0.01$.

3.4. Effect of HPOB on the Cort-induced dysfunction of the mitochondria

Given that HPOB inhibited Cort-induced mitochondrial GR translocation, we undertook a series of studies to investigate whether mitochondrial function was disturbed by the translocation of GR to this intracellular organelle and the effect of HPOB on this process. We first detected the influence of HPOB on the opening of the mitochondrial permeability transition pore (mPTP) using the calcein-cobalt quenching method. As shown in Fig. 4A and B, exposure to 250 μM Cort for 24 h significantly decreased green fluorescence (##$P<0.01$) compared to the control group, indicating cobalt quenching of calcein in the inner mitochondrial matrix and the profound release of calcein into the cytosol, which is consistent with mPTPs opening. In comparison, pre-treatment with HPOB (0.5 μM) blocked Cort-triggered decrease in green fluorescence intensity (**$P<0.01$), demonstrating HPOB induced the closure of mPTPs. Secondly, we further confirmed with JC-1 staining that HPOB reversed Cort-induced MMP depolarisation in PC12 cells. JC-1 accumulates in the mitochondria in a potential-dependent manner. In normal cells, JC-1 accumulates and forms dimeric J-aggregates in the mitochondria that give off a bright red fluorescence. However, when the potential is disturbed, the dye cannot access the transmembrane space and remains in the cytoplasm in its monomeric form, which gives off a bright green fluorescence. Consequently, mitochondrial depolarisation is indicated by a

decrease in the red/green fluorescence intensity ratio. As shown in Fig. 4C and D, Cort significantly decreased the red/green fluorescence intensity ratio (##P<0.01). However, HPOB (0.5 μM) prevented this decrease (**P<0.01). Thus, these results indicated that the HPOB-triggered inhibition of mitochondrial GR translocation was accompanied by the restoration of mitochondrial function.

Fig. 4. Effect of HPOB on Cort-induced dysfunction of the mitochondria. (A) HPOB treatment inhibited the Cort-induced opening of mPTP in PC12 cells. Cells were cultured in 24-well plates. After treatment, cells were loaded with calcein dye and incubated with cobalt chloride, and emission was measured at wavelengths of 488 and 505 nm. Reduced green fluorescence indicated calcein-cobalt quenching and opening of the mPTP. (B) The mPTP of cells in each group was calculated as the green fluorescence intensity analysed using a fluorescence microplate reader. (C) Effects of HPOB on MMP in Cort-induced PC12 cells. Representative fluorescence images of PC12 cells stained with the MMP-sensitive dye JC-1. Red fluorescence was due to JC-1 aggregates in healthy mitochondria with polarised inner mitochondrial membranes, while green fluorescence was emitted by cytosolic JC-1 monomers and indicated MMP dissipation. Merged images indicate co-localisation of JC-1 aggregates and monomers. (D) The MMP of cells in each group was calculated as the fluorescence ratio of red to green. The MMP was analysed using a fluorescence microplate reader after JC-1 staining. The results are expressed as a percentage of control. Cells were pre-incubated for 24 h with HPOB and then co-treated with Cort for 18 h. The untreated control group was incubated with the appropriate amount of vehicle. The results are expressed as the means ± SD of three independent experiments. ## indicates a significant difference from the control ($P < 0.01$). * indicates a significant difference from the treatment with Cort alone at $P < 0.05$. ** indicates a significant difference from treatment with Cort alone at $P < 0.01$. Scale bar: 100 μm.

3.5. Effect of HPOB on the intrinsic mitochondrial fission and apoptosis pathway in Cort-treated PC12 cells

To further explore the influence of HPOB on intrinsic mitochondrial fission and

apoptosis, the levels of pro-caspase-3, cleaved caspase-3 and released Cytochrome C (Cyto C) were measured (Fig. 5A). Furthermore, expression of Bax, MAP-1, Fis1, and DRP1 in mitochondrial fractions was also assessed to demonstrate the activation of the mitochondrial fission and intrinsic apoptosis pathway. Fig. 5B shows that HPOB significantly blocked the Cort-induced up-regulation of cleaved caspase-3, released Cyto C, and mitochondrial Fis1, DRP1, and Bax expression, indicating that HPOB reversed the mitochondrial fission and apoptotic pathway.

Fig. 5. Effects of HPOB on mitochondrial fission and the intrinsic apoptotic pathway in Cort-treated PC12 cells. (A) The effects of HPOB on the release of Cyto C and cleaved caspase-3 in Cort-treated PC12 cells. (B) Fis1, DRP1, MAP-1, and Bax expression in mitochondria was determined. HPOB treatment reversed the intrinsic mitochondrial pathway. Protein levels were quantified using densitometry. Cells were pre-incubated with HPOB for 24 h, and then co-treated with Cort for 18 h. The untreated control group was incubated with the appropriate amount of vehicle. The results are expressed as the means ± SD (n=3). ## indicates a significant difference from the control ($P < 0.01$). * indicates a significant difference from treatment with Cort alone at $P < 0.05$. ** indicates a significant difference from treatment with Cort alone at $P < 0.01$.

3.6. Effect of HPOB on the expression and acetylation of HDAC6-related molecular chaperones in Cort-treated PC12 cells

To analyse the mechanism by which HPOB influenced GR translocation to the mitochondria, we further examined the influence of selective HDAC6 inhibition on the heat shock protein family in Cort-induced apoptosis. First, we observed that exposure to Cort induced the up-regulation of HDAC6 but the down-regulation of Hsp90 and Hsp70 (Fig. 6A). HPOB treatment reversed these effects. In addition, Co-IP analysis revealed that HPOB triggered the increased acetylation of Hsp90 and Hsp70 compared with the control and Cort alone groups (Fig. 6A). We analysed the

acetylated lysine residues following HDAC6 knockdown via siRNA to confirm the crucial role of selective inhibition of HDAC6 by HPOB in the hyperacetylation of Hsp90 and Hsp70. The results showed that HDAC6 knockdown induced significant acetylation following HPOB treatment (Fig. 6B).

Fig. 6. (A) The effects of HPOB on Hsp90 and Hsp70 acetylation and Hsp90, Hsp70, and HDAC6 expression in Cort-treated PC12 cells. All of the experiments included control, HPOB, Cort and Cort plus HPOB groups and used β-actin as the loading control. (B) HPOB or HDAC6 siRNA induced HSP90 and HSP70 acetylation, proving that HDAC6 was involved in deacetylation of HSP90 and HSP70. PC12 cells were exposed to the HPOB and HDAC6 siRNA. The pellets were lysed, then HSP90 and HSP70 were immunoprecipitated from the lysates. Immunoblotting (IB) with an acetyl-lysine antibody was then performed. Protein levels were quantified using densitometry. Cells were pre-incubated with HPOB for 24 h and then co-treated with Cort for 18 h. The untreated control group was incubated with the appropriate amount of vehicle. The results are expressed as the means ± SD (n=3). ## indicates a significant difference from the control ($P < 0.01$). * indicates a significant difference from treatment with Cort alone at $P < 0.05$. ** indicates a significant difference from treatment with Cort alone at $P < 0.01$.

3.7. Effect of HPOB on mitochondrial preprotein transport in Cort-treated PC12 cells

To further elucidate the mechanism of HPOB interference in GR translocation to the mitochondria, we examined the levels of outer membrane mitochondrial translocation complexes (Tom). As shown in Fig. 7A, western blot analysis revealed that HPOB reversed Cort-induced elevation of Tom20 and Tom40 levels and unexpectedly up-regulated the levels of Tom70 and Hop. Furthermore, Co-IP results confirmed that HPOB attenuated Cort-induced binding of intracellular Tom70 and Hop to Hsp90, even though the expression levels of these two proteins were both elevated. To provide additional evidence, we isolated mitochondria with a mitochondrial fractionation kit (Invitrogen, Eugene, OR, USA) and performed western blotting to evaluate the levels of Tim22, Mia40, and mtHsp60 expression after HPOB

pre-treatment in Cort-treated cells. The results showed HPOB decreased the expression levels of Tim22, Mia40 and mtHsp60 (Fig. 7B). These observations suggest a model in which HPOB blocks the translocation of GR via the inhibition of HDAC6-mediated deacetylation of Hsp90, which obstructs its binding to translocation complexes.

Fig. 7. Effects of HPOB on the mitochondrial preprotein transport complex. (A) The effects of HPOB on Tom20, Tom40, Tom70, and Hop expression in total lysate from Cort-treated PC12 cells using western blot analysis. All of the experiments included control, HPOB, Cort and Cort plus HPOB groups and used β-actin as the loading control. HPOB blocked the binding of Tom70 and Hop to Hsp90. PC12 cells were exposed to HPOB, and Hsp90 was immunoprecipitated from the lysates, followed by detection of Tom70 and Hop using immunoblotting (IB) with Tom70 and Hop antibodies. (B) HPOB decreased the expression levels of Tim22, Mia40 and mtHsp60 in mitochondria. Protein expression levels were quantified using densitometry. Cells were pre-incubated with HPOB for 24 h, and then co-treated with Cort for 18 h. The untreated control group was incubated with the appropriate amount of vehicle. The results are expressed as the means ± SD (n=3). ## indicates a significant difference from the control ($P < 0.01$). * indicates a significant difference from treatment with Cort alone at $P < 0.05$. ** indicates a significant difference from treatment with Cort alone at $P < 0.01$.

Discussion

Numerous studies have demonstrated stress-induced increases in GC levels are positively correlated with atrophy of the hippocampus and major depression, and several lines of evidence have demonstrated a strong relationship between the reduction of hippocampal neurons and GC-induced apoptosis. According to the common theory of GC action, GR activation produces a genomic action through its association with several downstream effectors promoting expression of apoptogenic proteins that trigger the biochemical changes leading to cell death. Non-genomic GC effects, such as mitochondrial translocation of GR, have also been proved to mediate apoptosis in a nucleus-independent manner, in contrast to genomic GC action. Some

studies have indicated that treatment of cells with GCs causes mitochondrial translocation of GR and concomitant apoptosis, while inhibition of mitochondrial translocation attenuates Cort-induced cell death (Sionov et al., 2006a). The previous results further suggested regulation of HDAC6 might function as a target to influence mitochondrial GR translocation, thereby altering neuronal apoptosis (Li et al., 2014).

In the present study, we first confirmed that the selective HDAC6 inhibitor HPOB reversed Cort-induced damage to PC12 cells, and we further elucidated that the mechanism of this effect was probably correlated with the obstruction of Cort-induced mitochondrial GR translocation. HPOB pre-treatment reduced the levels of GR in mitochondria and enhanced the proportion of GR in the cytoplasm but did not substantially alter nuclear-directed GR translocation. It has been well established that the pro-apoptotic effects of Cort are primarily generated by mitochondrial GR translocation, and HPOB-mediated inhibition of GR intracellular trafficking to the mitochondria may play a significant role during neuroprotection.

Given the potential role of GR mitochondrial translocation in integrating the apoptotic signals in Cort-induced apoptosis (Sionov et al., 2006b; Tsiriyotis et al., 1997), we examined whether the inhibition of GR translocation was positively correlated with mitochondrial dysfunction and the intrinsic apoptosis pathway. First, we found HPOB reversed the excessive opening of mPTPs and depolarisation of MMP, which suggested repressing GR translocation restored mitochondrial functions. Then, we demonstrated HPOB decreased the levels of Fis1, Drp1, Map-1, and Bax in mitochondria, blocked Cyto c release, and reduced the proportion of cleaved caspase-3. Drp1 is ubiquitously expressed but most abundant in the skeletal muscle, heart, and brain (Varadi et al., 2004). During apoptosis, Drp1 assists in the conformational changes of Bax and facilitates its transmembrane translocation from the cytosol to mitochondria. Upon assembly in the mitochondrial membrane, Bax combines with its critical mitochondrial effector, MAP-1. MAP-1 is a mitochondria-enriched protein that associates with Bax only upon induction of apoptosis and initiates a death programme through a series of events culminating in the release of apoptogenic factors such as Cyto c. Translocated Drp1 localizes to

potential sites of mitochondria to promote organelle fission and affect mitochondria morphology (Jourdain et al., 2009; Wong et al., 2000). The expression level of Fis1 at the mitochondrial surface dictates the fission process. Specifically, Fis1 was shown to localize to the outer mitochondrial membrane and, in cooperation with Drp1, participate in mitochondrial fission (Breckenridge et al., 2008; Mai et al., 2010). Fragmentation of the mitochondrial network by Fis1 ultimately leads to Cyto C release and apoptosis, highlighting the critical role for these proteins in the intrinsic mitochondrial apoptotic pathway (Loson et al., 2013; Shen et al., 2014). Therefore, our results indicated HPOB might attenuate mitochondrial fission and activation of the intrinsic apoptotic pathway through blocking mitochondrial GR translocation.

To analyse the mechanism by which HPOB influenced GR translocation to the mitochondria, we focused on the role of HDAC6-mediated deacetylation. Abundant evidence has demonstrated that HDAC6 functions as a chaperone deacetylase, and inactivation of HDAC6 leads to the loss of chaperone activity via hyperacetylation. In addition, some researchers have shown that Hsps might function as interaction sites for the mitochondrial protein import receptor translocase of the outer membrane 70 (Tom70) (Williams and Nelsen, 1997; Young et al., 2003). Hsps are a family of conserved molecular chaperones that perform versatile functions, such as preventing aggregation of nascent polypeptide chains, post-translational targeting of proteins and assisting in protein conformation folding (Lim et al., 2005; Richter and Buchner, 2001; Weis et al., 2010). Some recent studies have proposed that Hsps also act as cytosolic transport factors. In particular, Hsp70 and Hsp90, the major members of the Hsp family that are central to chaperone-dependent lysosomal import, have been shown to participate in mitochondrial import pathways (Young et al., 2003). As shown in Fig. 6A, our results revealed that HPOB triggered the hyperacetylation of Hsp70 and Hsp90 and reversed Cort-induced up-regulation of HDAC6 and reduction of Hsp70 and Hsp90. Both HPOB treatment and the knockdown of HDAC6 protein levels using siRNA resulted in the hyperacetylation of Hsp90 and Hsp70 (Fig. 6B). These results implied that HPOB-mediated acetylation of Hsps might be involved in both the trafficking and mitochondrial translocation of GR and further play a crucial role in

blocking Cort-induced apoptosis.

During mitochondrial protein transport, Tom act as a gateway (Muro et al., 2003), and these complexes are primarily composed of Tom20, Tom40, and Tom70. Tom20 recognizes the classical N-terminal amphipathic mitochondrial-targeting pre-sequence of the precursor protein. Tom70, another receptor, recognizes pre-proteins with targeting signals embedded in their internal sequences (Beddoe et al., 2004; Wiedemann et al., 2004). After binding to the receptors, pre-proteins are transferred to Tom40, a channel-forming protein that is the major component of the general import pore (GIP). Pre-proteins are further sorted by inner membrane translocation machinery (Tim) (Chacinska et al., 2003; Chacinska et al., 2010). Remarkably, it was found that Tom70-recognized pre-proteins in the cytosol were associated with a multi-chaperone complex including Hsp90 and Hsp70 in mammals. The docking of Hsp90 onto the clamp region of Tom70 was necessary for the efficient recognition of internal targeting sequences in the pre-protein by the Tom70 core domain. In addition, Hsp90 was reported to cooperate with Hsp70 via Hsp70/Hsp90-organizing protein (Hop), which is the functional link between the two molecular chaperones. As a junction adaptor protein, Hop may participate in the initial formation of the multi-chaperone complex but is then generally displaced by the docking of Hsp90 onto Tom70 (Chen et al., 1996; Scheufler et al., 2000). These data suggest that the translocation complexes of outer membrane and Hsp70/Hsp90-organizing proteins may guide GR mitochondrial translocation (Brinker et al., 2002). We therefore determined the HPOB-induced influence of Tom20, Tom40, Tom70, and Hop in Cort-treated PC12 cells. As shown in Fig. 6A, our results revealed that HPOB attenuated the Cort-induced increase in Tom20 and Tom40 expression and unexpectedly up-regulated the expression levels of Tom70 and Hop. Although Tom70 and Hop levels were up-regulated, co-IP experiments demonstrated a rapid decline in Cort-induced binding of intracellular Tom70 and Hop to Hsp90 following HPOB treatment. These observations may be explained by the hypothesis that HPOB blocking of Hsp90 binding to Tom70 and Hop initiates the compensatory up-regulation of these two proteins. It has also been reported that when the

multi-chaperone complex delivers the cargo to Tom70, Tom20 modulates the translocation of the cargo proteins across the translocon formed by Tom40. This suggests that when HPOB blocks the transport and binding between the multi-chaperone complex and Tom70, a compensatory down-regulation of Tom20 and Tom40 may also occur. Furthermore, our results implied that the HPOB-induced elevation of Tom70 and Hop levels did not counteract the influence of the inhibition of Hsp90 binding. In addition, chaperone carrier proteins destined for the mitochondrial matrix were shown to be translocated across the inner mitochondrial membrane (IM) through a translocon formed by the transporter of the Tim22 complex (Rassow et al., 1999; Rassow and Pfanner, 2000; Voos et al., 1999). The Tim complex further interacts with the mitochondrial heat shock proteins (mtHsps) that hydrolyse ATP to pull the cargo protein into the mitochondrial matrix (Glick, 1995; Voisine et al., 1999). Moreover, precursor proteins that remain in the intermembrane space (IMS) are specifically recognized by receptor Mia40 (Bragoszewski et al., 2015), which catalyses the refolding of precursor proteins with the help of mtHsp60. This provides a trapping mechanism that prevents the escape of proteins from the IMS back to the cytosol (Bomer et al., 1998; Voos et al., 1996). Therefore, we determined the effect of HPOB on Tim22, Mia40 and mtHsp60. As expected, HPOB attenuated the expression levels of these cofactors, and this effect might be regarded as an adaptive response to reduced cargo protein, such as GR or other mitochondria-directed pre-proteins. This alteration also confirmed reduced localization of GR in the mitochondrial matrix from another side. Interestingly, the results also indicated treatment with HPOB alone decreased the levels of Tim22, Mia40, and mtHsp60 compared with the control group, implying excessive acetylation might obstruct mitochondrial localization of Hsps. As noted above, HPOB treatment resulted in the acetylation of Hsp90 and Hsp70. This effect likely reduced Hsp90 cooperation with Hsp70 via their functional link. Moreover, acetylated Hsp90 may be unable to bind to the clamp region of Tom70, thereby decreasing the formation of mitochondrial translocation complexes on the outer membrane and preventing transmembrane transport of GR.

In conclusion, our present work highlighted that the selective inhibition of HDAC6

could be a therapeutic target against GC-induced apoptosis through blocking the mitochondrial translocation of GR and the subsequent mitochondrial dysfunction and activation of the intrinsic apoptosis pathway. To elucidate this process, we focused on the HDAC6-mediated post-translational modifications of Hsps. The results revealed that selectively inhibiting HDAC6 caused hyperacetylation of Hsp90 and Hsp70, thereby triggering rapid decline in the binding of intracellular Tom70 and Hop to Hsp90 and leading to restricted formation of the multi-chaperone translocation system that ultimately blocked mitochondrial GR translocation. Furthermore, HPOB reversed Cort-induced attenuation of Hsp90 and Hsp70 expression, two molecular chaperones that might function complementarily or collaboratively to block Cort-mediated apoptosis. Thus, our present study provided a substantial foundation for illuminating the mechanisms of the HPOB-mediated neuroprotective effect against GC-induced apoptosis. By establishing a potential link between the selective inhibition of HDAC6 and GC-related chronic stress, the current study solidifies HPOB as a possible candidate for mitigating stress-induced neurotoxicity during major depression. Admittedly, future experiments are required to evaluate and elucidate the anti-apoptotic efficacy of HPOB and demonstrate the feasibility of selective HDAC6 inhibitors as neuroprotective agents against GC-induced apoptosis.

Acknowledgements

This project was supported by the Research Fund from Shenzhen Key Laboratory of Neurosurgery (ZDSYS20140509173142601), Basic research projects of Shenzhen Science and Technology Program (JCYJ20150306114616, JCYJ20150330102720152 and JCYJ2920831101643895) and the Natural Science Foundation of Guangdong (2014A030310057)

Conflict of interest

No potential conflicts of interest (financial or non-financial) were declared.

Reference

Adzic, M., Djordjevic, A., Demonacos, C., Krstic-Demonacos, M., Radojcic, M.B., 2009. The role of phosphorylated glucocorticoid receptor in mitochondrial functions and apoptotic signalling in brain tissue of stressed Wistar rats. Int J Biochem Cell Biol 41, 2181-2188.

Beddoe, T., Bushell, S.R., Perugini, M.A., Lithgow, T., Mulhern, T.D., Bottomley, S.P., Rossjohn, J., 2004. A biophysical analysis of the tetratricopeptide repeat-rich mitochondrial import receptor, Tom70, reveals an elongated monomer that is inherently flexible, unstable, and unfolds via a multistate pathway. J Biol Chem 279, 46448-46454.

Bomer, U., Maarse, A.C., Martin, F., Geissler, A., Merlin, A., Schonfisch, B., Meijer, M., Pfanner, N., Rassow, J., 1998. Separation of structural and dynamic functions of the mitochondrial translocase: Tim44 is crucial for the inner membrane import sites in translocation of tightly folded domains, but not of loosely folded preproteins. EMBO J 17, 4226-4237.

Bragoszewski, P., Wasilewski, M., Sakowska, P., Gornicka, A., Bottinger, L., Qiu, J., Wiedemann, N., Chacinska, A., 2015. Retro-translocation of mitochondrial intermembrane space proteins. Proc Natl Acad Sci U S A 112, 7713-7718.

Breckenridge, D.G., Kang, B.H., Kokel, D., Mitani, S., Staehelin, L.A., Xue, D., 2008. Caenorhabditis elegans drp-1 and fis-2 regulate distinct cell-death execution pathways downstream of ced-3 and independent of ced-9. Mol Cell 31, 586-597.

Brinker, A., Scheufler, C., Von Der Mulbe, F., Fleckenstein, B., Herrmann, C., Jung, G., Moarefi, I., Hartl, F.U., 2002. Ligand discrimination by TPR domains. Relevance and selectivity of EEVD-recognition in Hsp70 x Hop x Hsp90 complexes. J Biol Chem 277, 19265-19275.

Chacinska, A., Rehling, P., Guiard, B., Frazier, A.E., Schulze-Specking, A., Pfanner, N., Voos, W., Meisinger, C., 2003. Mitochondrial translocation contact sites: separation of dynamic and stabilizing elements in formation of a TOM-TIM-preprotein supercomplex. EMBO J 22, 5370-5381.

Chacinska, A., van der Laan, M., Mehnert, C.S., Guiard, B., Mick, D.U., Hutu, D.P., Truscott, K.N., Wiedemann, N., Meisinger, C., Pfanner, N., Rehling, P., 2010. Distinct forms of mitochondrial TOM-TIM supercomplexes define signal-dependent states of preprotein sorting. Mol Cell Biol 30, 307-318.

Chen, S., Prapapanich, V., Rimerman, R.A., Honore, B., Smith, D.F., 1996. Interactions of p60, a mediator of progesterone receptor assembly, with heat shock proteins hsp90 and hsp70. Mol Endocrinol 10, 682-693.

Demonacos, C., Djordjevic-Markovic, R., Tsawdaroglou, N., Sekeris, C.E., 1995. The mitochondrion as a primary site of action of glucocorticoids: the interaction of the glucocorticoid receptor with mitochondrial DNA sequences showing partial similarity to the nuclear glucocorticoid responsive elements. J Steroid Biochem Mol Biol 55, 43-55.

Du, J., Wang, Y., Hunter, R., Wei, Y., Blumenthal, R., Falke, C., Khairova, R., Zhou, R., Yuan, P., Machado-Vieira, R., McEwen, B.S., Manji, H.K., 2009. Dynamic regulation of mitochondrial function by glucocorticoids. Proc Natl Acad Sci U S A 106, 3543-3548.

Glick, B.S., 1995. Pathways and energetics of mitochondrial protein import in Saccharomyces cerevisiae. Methods Enzymol 260, 224-231.

He, Y., Szapary, D., Simons, S.S., Jr., 2002. Modulation of induction properties of glucocorticoid receptor-agonist and -antagonist complexes by coactivators involves binding to receptors but is

independent of ability of coactivators to augment transactivation. J Biol Chem 277, 49256-49266.

Jourdain, I., Gachet, Y., Hyams, J.S., 2009. The dynamin related protein Dnm1 fragments mitochondria in a microtubule-dependent manner during the fission yeast cell cycle. Cell Motil Cytoskeleton 66, 509-523.

Kovacs, J.J., Murphy, P.J., Gaillard, S., Zhao, X., Wu, J.T., Nicchitta, C.V., Yoshida, M., Toft, D.O., Pratt, W.B., Yao, T.P., 2005. HDAC6 regulates Hsp90 acetylation and chaperone-dependent activation of glucocorticoid receptor. Mol Cell 18, 601-607.

Lee, J.H., Mahendran, A., Yao, Y., Ngo, L., Venta-Perez, G., Choy, M.L., Kim, N., Ham, W.S., Breslow, R., Marks, P.A., 2013. Development of a histone deacetylase 6 inhibitor and its biological effects. Proc Natl Acad Sci U S A 110, 15704-15709.

Li, Z.Y., Jiang, Y.M., Liu, Y.M., Guo, Z., Shen, S.N., Liu, X.M., Pan, R.L., 2014. Saikosaponin D acts against corticosterone-induced apoptosis via regulation of mitochondrial GR translocation and a GR-dependent pathway. Prog Neuropsychopharmacol Biol Psychiatry 53, 80-89.

Lim, S.O., Park, S.G., Yoo, J.H., Park, Y.M., Kim, H.J., Jang, K.T., Cho, J.W., Yoo, B.C., Jung, G.H., Park, C.K., 2005. Expression of heat shock proteins (HSP27, HSP60, HSP70, HSP90, GRP78, GRP94) in hepatitis B virus-related hepatocellular carcinomas and dysplastic nodules. World J Gastroenterol 11, 2072-2079.

Loson, O.C., Song, Z., Chen, H., Chan, D.C., 2013. Fis1, Mff, MiD49, and MiD51 mediate Drp1 recruitment in mitochondrial fission. Mol Biol Cell 24, 659-667.

Mai, S., Klinkenberg, M., Auburger, G., Bereiter-Hahn, J., Jendrach, M., 2010. Decreased expression of Drp1 and Fis1 mediates mitochondrial elongation in senescent cells and enhances resistance to oxidative stress through PINK1. J Cell Sci 123, 917-926.

Maiyar, A.C., Phu, P.T., Huang, A.J., Firestone, G.L., 1997. Repression of glucocorticoid receptor transactivation and DNA binding of a glucocorticoid response element within the serum/glucocorticoid-inducible protein kinase (sgk) gene promoter by the p53 tumor suppressor protein. Mol Endocrinol 11, 312-329.

Mikosz, C.A., Brickley, D.R., Sharkey, M.S., Moran, T.W., Conzen, S.D., 2001. Glucocorticoid receptor-mediated protection from apoptosis is associated with induction of the serine/threonine survival kinase gene, sgk-1. J Biol Chem 276, 16649-16654.

Moutsatsou, P., Psarra, A.M., Tsiapara, A., Paraskevakou, H., Davaris, P., Sekeris, C.E., 2001. Localization of the glucocorticoid receptor in rat brain mitochondria. Arch Biochem Biophys 386, 69-78.

Muro, C., Grigoriev, S.M., Pietkiewicz, D., Kinnally, K.W., Campo, M.L., 2003. Comparison of the TIM and TOM channel activities of the mitochondrial protein import complexes. Biophys J 84, 2981-2989.

Namdar, M., Perez, G., Ngo, L., Marks, P.A., 2010. Selective inhibition of histone deacetylase 6 (HDAC6) induces DNA damage and sensitizes transformed cells to anticancer agents. Proc Natl Acad Sci U S A 107, 20003-20008.

Psarra, A.M., Sekeris, C.E., 2011. Glucocorticoids induce mitochondrial gene transcription in HepG2 cells: role of the mitochondrial glucocorticoid receptor. Biochim Biophys Acta 1813, 1814-1821.

Rao, R., Fiskus, W., Ganguly, S., Kambhampati, S., Bhalla, K.N., 2012. HDAC inhibitors and chaperone function. Adv Cancer Res 116, 239-262.

Rassow, J., Dekker, P.J., van Wilpe, S., Meijer, M., Soll, J., 1999. The preprotein translocase of the

mitochondrial inner membrane: function and evolution. J Mol Biol 286, 105-120.

Rassow, J., Pfanner, N., 2000. The protein import machinery of the mitochondrial membranes. Traffic 1, 457-464.

Richter, K., Buchner, J., 2001. Hsp90: chaperoning signal transduction. J Cell Physiol 188, 281-290.

Ryhanen, T., Viiri, J., Hyttinen, J.M., Uusitalo, H., Salminen, A., Kaarniranta, K., 2011. Influence of Hsp90 and HDAC inhibition and tubulin acetylation on perinuclear protein aggregation in human retinal pigment epithelial cells. J Biomed Biotechnol 2011, 798052.

Sapolsky, R.M., 2000. Glucocorticoids and hippocampal atrophy in neuropsychiatric disorders. Arch Gen Psychiatry 57, 925-935.

Savoldi, G., Fenaroli, A., Ferrari, F., Rigaud, G., Albertini, A., Di Lorenzo, D., 1997. The glucocorticoid receptor regulates the binding of C/EPBbeta on the alpha-1-acid glycoprotein promoter in vivo. DNA Cell Biol 16, 1467-1476.

Scheufler, C., Brinker, A., Bourenkov, G., Pegoraro, S., Moroder, L., Bartunik, H., Hartl, F.U., Moarefi, I., 2000. Structure of TPR domain-peptide complexes: critical elements in the assembly of the Hsp70-Hsp90 multichaperone machine. Cell 101, 199-210.

Shen, Q., Yamano, K., Head, B.P., Kawajiri, S., Cheung, J.T., Wang, C., Cho, J.H., Hattori, N., Youle, R.J., van der Bliek, A.M., 2014. Mutations in Fis1 disrupt orderly disposal of defective mitochondria. Mol Biol Cell 25, 145-159.

Sionov, R.V., Cohen, O., Kfir, S., Zilberman, Y., Yefenof, E., 2006a. Role of mitochondrial glucocorticoid receptor in glucocorticoid-induced apoptosis. J Exp Med 203, 189-201.

Sionov, R.V., Kfir, S., Zafrir, E., Cohen, O., Zilberman, Y., Yefenof, E., 2006b. Glucocorticoid-induced apoptosis revisited: a novel role for glucocorticoid receptor translocation to the mitochondria. Cell Cycle 5, 1017-1026.

Tang, V.M., Young, A.H., Tan, H., Beasley, C., Wang, J.F., 2013. Glucocorticoids increase protein carbonylation and mitochondrial dysfunction. Horm Metab Res 45, 709-715.

Tsiriyotis, C., Spandidos, D.A., Sekeris, C.E., 1997. The mitochondrion as a primary site of action of glucocorticoids: mitochondrial nucleotide sequences, showing similarity to hormone response elements, confer dexamethasone inducibility to chimaeric genes transfected in LATK- cells. Biochem Biophys Res Commun 235, 349-354.

Varadi, A., Johnson-Cadwell, L.I., Cirulli, V., Yoon, Y., Allan, V.J., Rutter, G.A., 2004. Cytoplasmic dynein regulates the subcellular distribution of mitochondria by controlling the recruitment of the fission factor dynamin-related protein-1. J Cell Sci 117, 4389-4400.

Voisine, C., Craig, E.A., Zufall, N., von Ahsen, O., Pfanner, N., Voos, W., 1999. The protein import motor of mitochondria: unfolding and trapping of preproteins are distinct and separable functions of matrix Hsp70. Cell 97, 565-574.

Voos, W., Martin, H., Krimmer, T., Pfanner, N., 1999. Mechanisms of protein translocation into mitochondria. Biochim Biophys Acta 1422, 235-254.

Voos, W., von Ahsen, O., Muller, H., Guiard, B., Rassow, J., Pfanner, N., 1996. Differential requirement for the mitochondrial Hsp70-Tim44 complex in unfolding and translocation of preproteins. EMBO J 15, 2668-2677.

Weis, F., Moullintraffort, L., Heichette, C., Chretien, D., Garnier, C., 2010. The 90-kDa heat shock protein Hsp90 protects tubulin against thermal denaturation. J Biol Chem 285, 9525-9534.

Wiedemann, N., Truscott, K.N., Pfannschmidt, S., Guiard, B., Meisinger, C., Pfanner, N., 2004. Biogenesis of the protein import channel Tom40 of the mitochondrial outer membrane:

intermembrane space components are involved in an early stage of the assembly pathway. J Biol Chem 279, 18188-18194.

Williams, N.E., Nelsen, E.M., 1997. HSP70 and HSP90 homologs are associated with tubulin in hetero-oligomeric complexes, cilia and the cortex of Tetrahymena. J Cell Sci 110 (Pt 14), 1665-1672.

Wong, E.D., Wagner, J.A., Gorsich, S.W., McCaffery, J.M., Shaw, J.M., Nunnari, J., 2000. The dynamin-related GTPase, Mgm1p, is an intermembrane space protein required for maintenance of fusion competent mitochondria. J Cell Biol 151, 341-352.

Young, J.C., Hoogenraad, N.J., Hartl, F.U., 2003. Molecular chaperones Hsp90 and Hsp70 deliver preproteins to the mitochondrial import receptor Tom70. Cell 112, 41-50.

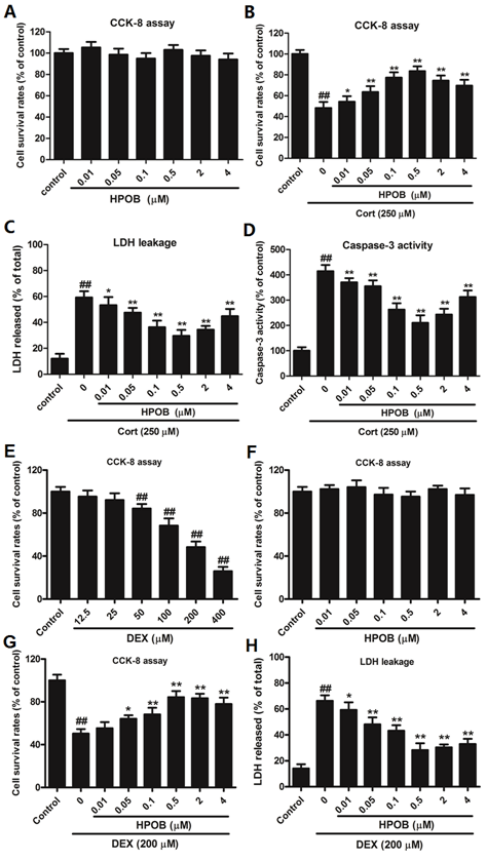

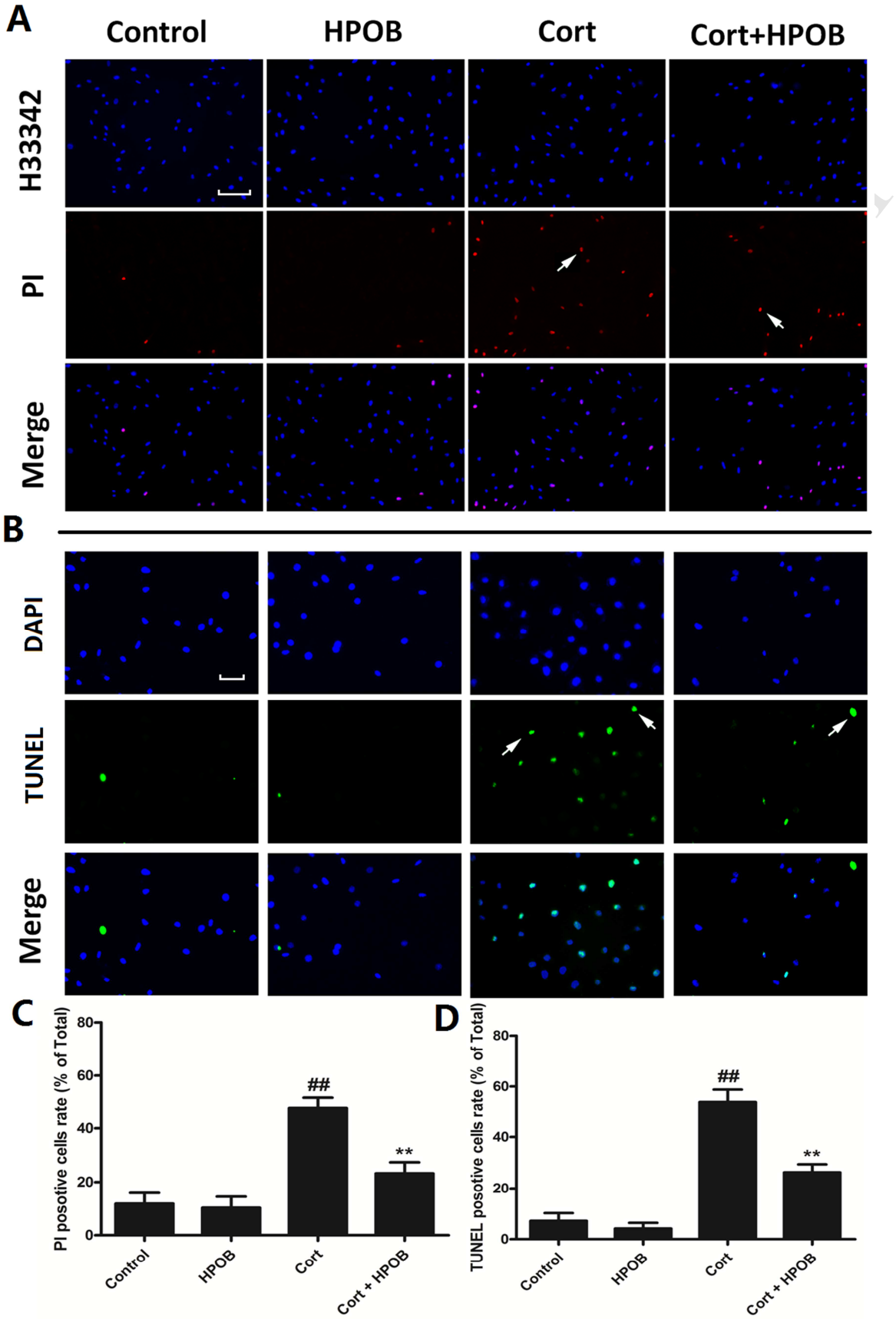
A
Control
HPOB
Cort
Cort+HPOB
H33342
PI
Merge
B
DAPI
TUNEL
Merge
C
PI posotive cells rate (% of Total)
80
60
40
20
0
##
**
Control
HPOB
Cort
Cort + HPOB
D
TUNEL posotive cells rate (% of Total)
80
60
40
20
0
##
**
Control
HPOB
Cort
Cort + HPOB

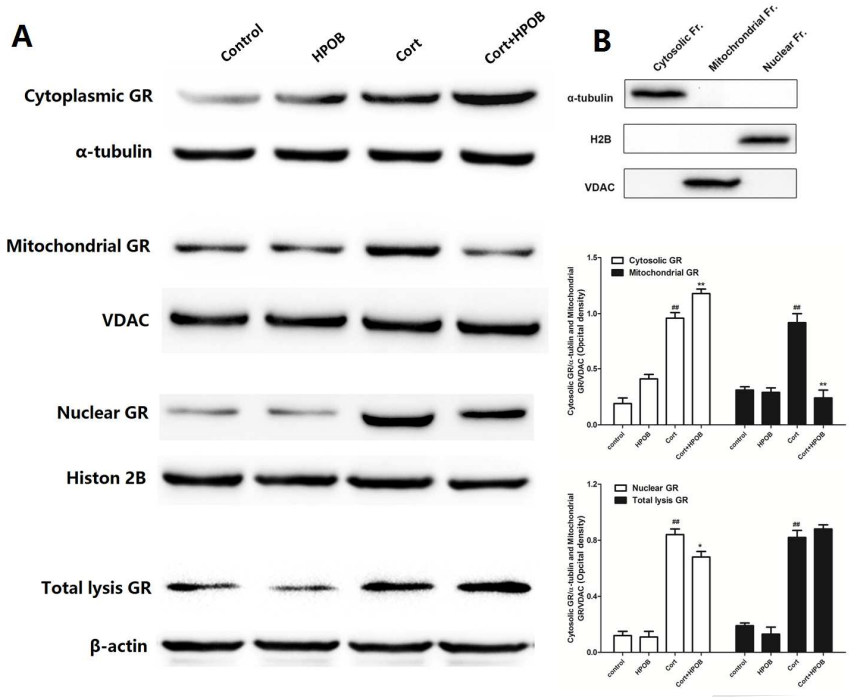

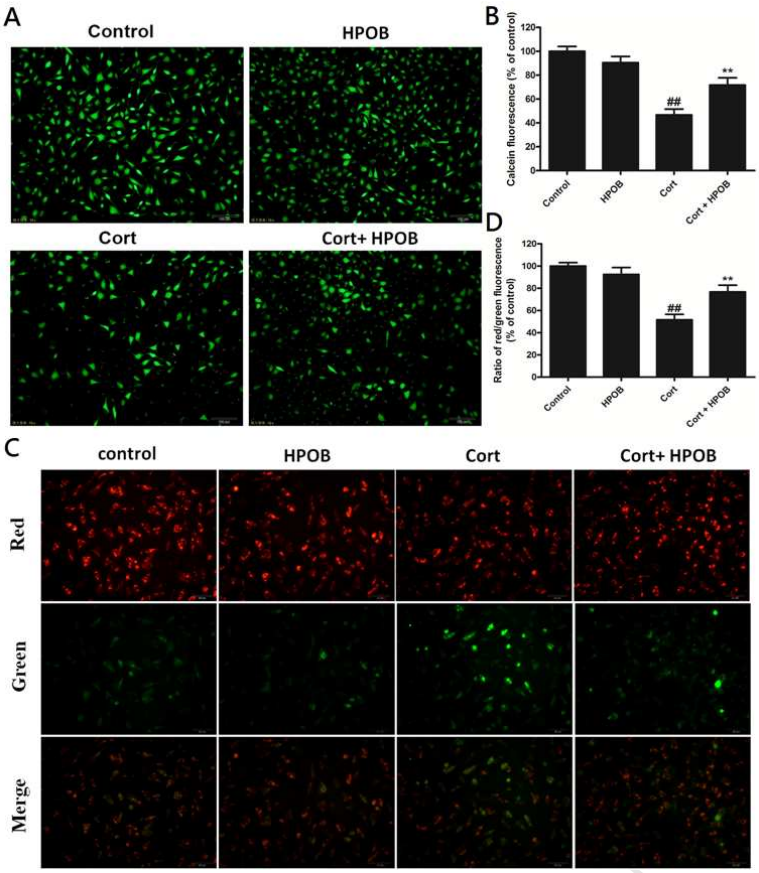

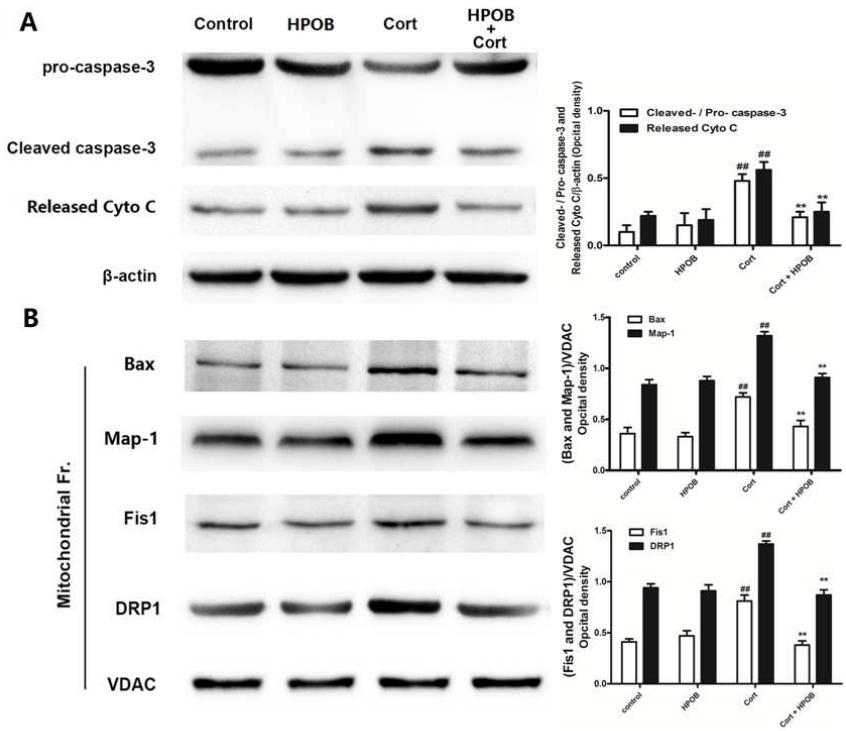

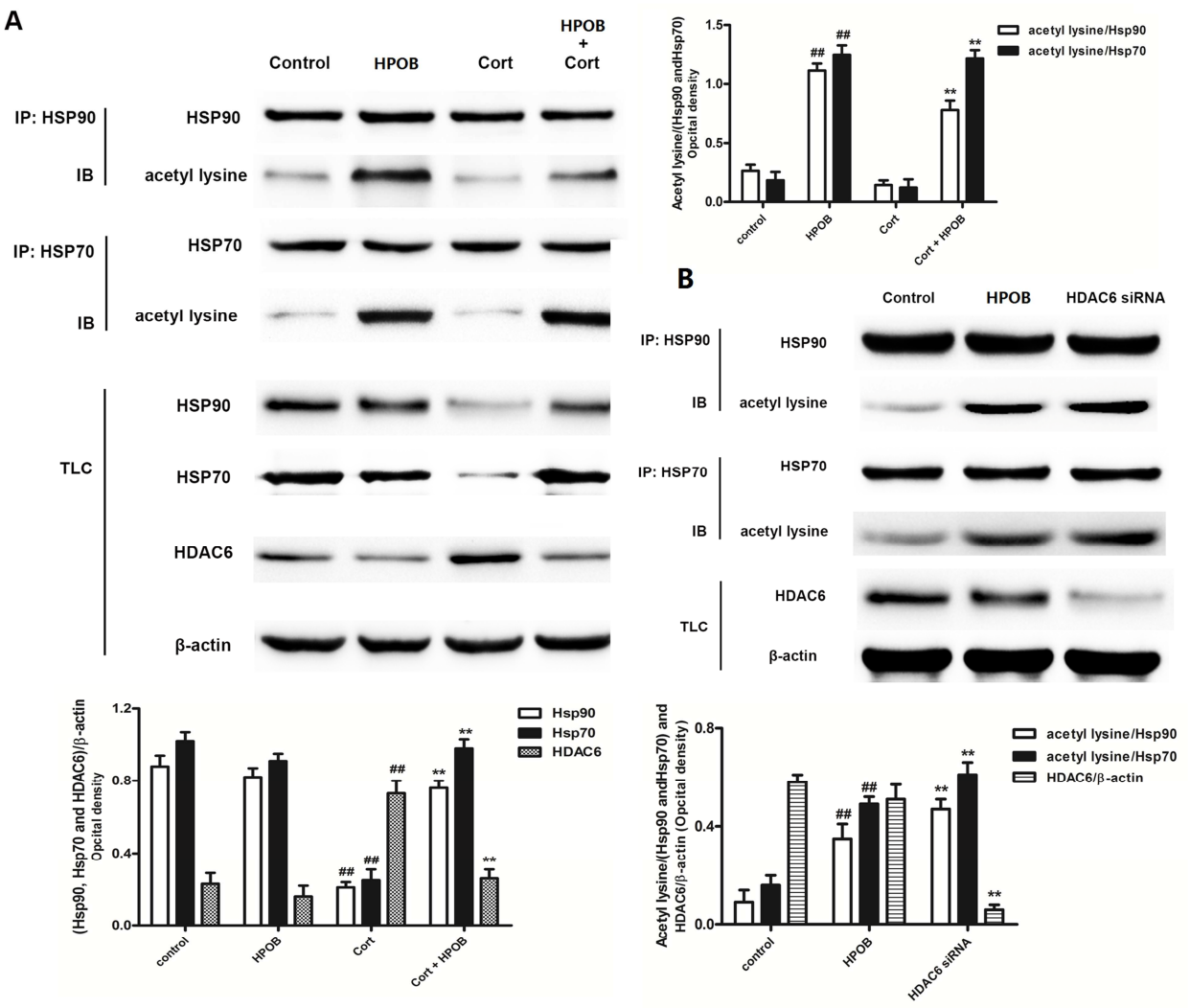
A
Control
HPOB
Cort
HPOB + Cort
IP: HSP90
HSP90
IB
acetyl lysine
IP: HSP70
HSP70
IB
acetyl lysine
TLC
HSP90
HSP70
HDAC6
β-actin
Acetyl lysine/(Hsp90 andHsp70) Opcital density
acetyl lysine/Hsp90
acetyl lysine/Hsp70
control
HPOB
Cort
Cort + HPOB
B
Control
HPOB
HDAC6 siRNA
IP: HSP90
HSP90
IB
acetyl lysine
IP: HSP70
HSP70
IB
acetyl lysine
TLC
HDAC6
β-actin
(Hsp90, Hsp70 and HDAC6)/β-actin Opcital density
Hsp90
Hsp70
HDAC6
Acetyl lysine/(Hsp90 andHsp70) and HDAC6/β-actin (Opcital density)
acetyl lysine/Hsp90
acetyl lysine/Hsp70
HDAC6/β-actin
HDAC6 siRNA

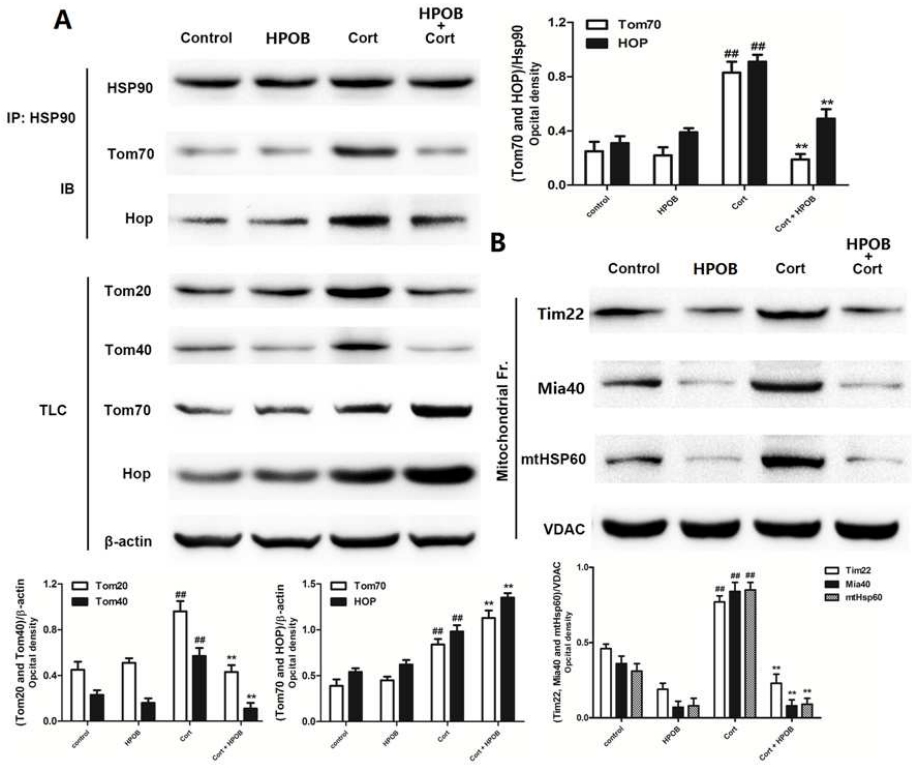

- HPOB (a selective HDAC6 inhibitor) attenuated corticosterone (Cort)-induced apoptosis.
- HPOB blocked Cort-caused mitochondrial GR translocation and followed apoptotic pathway.
- HPOB caused hyperacetylation of Hsps, thus triggering decline in the binding of Hop to Hsp90.
- HPOB attenuated the chaperone-depended mitochondrial transport with TOM/TIM complex.
- This work established a potential link between inhibition of HDAC6 and GC-related chronic stress.